Pergamon

Cement and Concrete Research 31 (2001) 1017–1021

CEMENT AND CONCRETE RESEARCH

Deteriorated pavements due to the alkali–silica reaction A petrographic study of three cases in Argentina

S.A. Marfil*[,1], P.J. Maiza[2]

Geology Department, Universidad Nacional del Sur, San Juan 670, 8000 Bahía Blanca, Argentina

Received 5 May 2000; accepted 15 March 2001

Abstract

Deteriorated concrete pavements from three regions in Argentina were studied. The aim was to evaluate aggregate constituents, especially the presence of deleterious components, determine what reaction products had developed, and find the main causes of the deterioration based on the petrographic study of the concrete. Thin sections were analyzed with a petrographic microscope to evaluate microcracking, characteristics of the aggregate–cement interface, reaction rims, and the development of reaction products. The latter were analyzed by X-ray diffraction (XRD), scanning electron microscopy (SEM), and energy dispersive X-ray analysis (EDAX). Pavements exhibit widespread microcracking with the development of crystalline materials at the aggregate rims, identified as zeolite-like structures by XRD. From the EDAX analysis, Si, Al, O, Ca, K, and Na were determined. Ettringite is abundant both inside cavities and on crack surfaces within concrete. Its occurrence was confirmed by XRD and EDAX. The aggregate deleterious constituents are mainly glassy vulcanites and volcanic glass, generally altered to argillaceous minerals, and strained quartz, with undulatory extinction. The deterioration of the three pavements studied was due to the development of the alkali–silica reaction (ASR), involving the strained quartz.

Keywords: Petrography; Alkali–aggregate reaction

1. Introduction

In Argentina, there is an increasing number of regions across the country where civil engineering works experience deterioration problems as a result of the alkali–silica reaction (ASR).

Previous studies focused on concrete used in dams, airports, and roads [1]. Deteriorated concretes show white exudates. This product was identified as zeolite-like structures, responsible for concrete expansion and cracking [2,3].

It is quite common to find ettringite associated with these ASR products [4–6].

The aim of the work described in this paper was to identify the reaction products that had developed and to determine the deterioration causes of different concrete pavements by a petrographic study.

Cole et al. [7] determined that the ASR product is a crystalline material similar to an artificial zeolite whose chemical composition is $(NaAlSiO_4)_{12}\cdot 27H_2O$ or $Ca(AlSiO_4)_{12}\cdot 27H_2O$. By X-ray diffraction (XRD), they obtained a very high reflection at 12.20 Å. This material was then heated at 110°C, which turned it into another one with a totally different structure. These authors report that the Al content of the material studied is very low. In 1983, Cole and Lancucki [8] compared the dehydrated product of their former work [7] to okenite, which has very clear reflections at 8.85, 3.5, 3.35, 2.98, 10.05, and 1.82 Å. This material was not identified in our work since the above reflections were not found.

In a former work [9], to crystallize ASR products, a silica (tridymite) sample in an alkaline state, with no aluminum, was subjected to physicochemical conditions of synthesis. A zeolitic structure, determined by XRD and electron diffraction as Na–P zeolite, was obtained.

* Corresponding author. Tel.: +54-291-459-5184; fax: +54-291-459-5148.

E-mail address: smarfil@criba.edu.ar (S.A. Marfil).

[1] Researcher at the Comisión de Investigaciones Científicas de la Provincia de Buenos Aires (CIC).

[2] Researcher at the Consejo Nacional de Investigaciones Científicas y Técnicas (CONICET).

0008-8846/01/$ – see front matter
PII: S0008-8846(01)00508-7

2. Methods

An Olympus SZ-Pt trinocular stereomicroscope, an Olympus B2-UMA trinocular petrographic microscope, both equipped with a built-in Sony video camera with a digital capture system, a JEOL JSM 35 CP scanning electron microscope, equipped with an energy dispersive X-ray analysis (EDAX) probe, DX4 with an ultrathin window with a range of analysis from $Z=5$ to $Z=92$, and a computer-based Rigaku X-ray diffractometer D-max III-C, 35 kV and 15 mA, with Cu Kα radiation and a monochromator of curved single crystal (graphite) were used.

3. Experimental

Concrete cores from three different regions in Argentina, called A, B, and C, were taken.

Concrete A:

A highway from the Province of Córdoba, 3 years old.

Concrete B:

Pavement of a road in the north of the Province of Buenos Aires, 18 years old.

Concrete C:

An urban road surface in the city of Bahía Blanca (in the south of the Province of Buenos Aires) built 15 years ago.

3.1. Stereomicroscope observations

The three pavements studied have experienced a strong deterioration process that influences concrete physical characteristics, texture, and compactness. Microcracking is significant and reaction products are abundant, mainly inside air voids, in open spaces, at the aggregate–paste interface. A coarse aggregate particle from the highway pavement affected by a significant alteration process is shown in Fig. 1A. A section of Concrete B, affected by a reaction process involving the particles and mortar, is depicted in Fig. 1B.

Two products can be identified in the reaction: one that is white, massive, opaque, and hard, which is related to erionite ($KNaCa(Si_{14}Al_4)O_{36}\cdot 8H_2O$) (Fig. 1C), and another that is white, bright, very soft, with a fibrous habit, which associated with ettringite (Fig. 1D). Both materials were extracted to be subjected to XRD, scanning electron microscopy (SEM), and EDAX analyses.

3.2. X-ray diffraction

The diffractogram of the fibrous material taken from the interior of air voids and the concrete surface is presented in Fig. 1E. Identified as ettringite (e) ($Ca_6Al_2(SO_4)_3(OH)_{12}\cdot 26H_2O$) (ICDD 41-1451), this mineral has the maximum intensity reflection at 9.72 Å. There is a lesser proportion of portlandite (p) and calcite (c).

Fig. 1F illustrates the XRD pattern of the white massive material observed in Fig. 1C extracted from the reactive aggregate–mortar interface and the interior of cracks. It was identified as a zeolite-like structure. Major reflections appear at 11.56, 3.56, 3.32, and 2.85 Å. They are the same as those of erionite and similar to those reported in ICDD 39-1379.

Although there is a discrepancy in the Al contents of the ASR product and erionite, in previous studies (op. cit.) zeolitic structures with almost no aluminum were synthesized in laboratory tests. Aluminum-free reaction products are reported in the literature [7,8]. The material found in the concrete studied cannot be identified as okenite because its XRD spectrum is different. There is also no erionite due to lack of Al in its composition. The exact pattern of the crystalline ASR product may not match that of any natural mineral.

3.3. Scanning electron microscopy–energy dispersive X-ray analysis

Fig. 2A illustrates the fibrous habit of ettringite formation within cavities and on the concrete surface. The EDAX analysis identified S, Al, O, and Ca (Fig. 2B).

The reactive aggregate particles of pavement C are surrounded by a white, hard material of a massive appearance that, towards the outside boundary (interface with the mortar), becomes transparent and of a gel-like appearance. SEM–EDAX analyses were performed from the boundary to the center. The gel appearance of the transparent product is depicted in Fig. 2C. Si, Al, O, and Ca were identified (Fig. 2D). Although Al is rarely observed in alkali–silica gels, it has been identified in rosette-like crystals [10,11].

Within aggregate boundary, the AAR product exhibits a crystalline habit, as shown in Fig. 2E. The chemical composition is Si, O, Ca, Na, and K (Fig. 2F). Although it has no Al, this material was attributed to a zeolite-like structure. There are a large number of ICDD cards [12] that classify zeolitic structures with no aluminum. Cole (op. cit.) also determined aluminum-free reaction products and identified them first as zeolites (natural sample) and then as okenite (dehydrated material). The XRD spectrum of this mineral does not agree with that of the material studied in our work. The crystallographic properties of the crystalline AAR products need further studies.

3.4. Petrographic microscopy

3.4.1. Aggregate characteristics

The aggregates contained in the concrete, especially the deleterious components, were observed with the petrographic microscope on thin sections:

Concrete A:

The coarse aggregate consists mainly of quartz rocks containing microcrystalline quartz, with mortar textures and undulatory extinction (UE angle$\cong$11°). Embayed quartz and reaction rims are noticeable at the

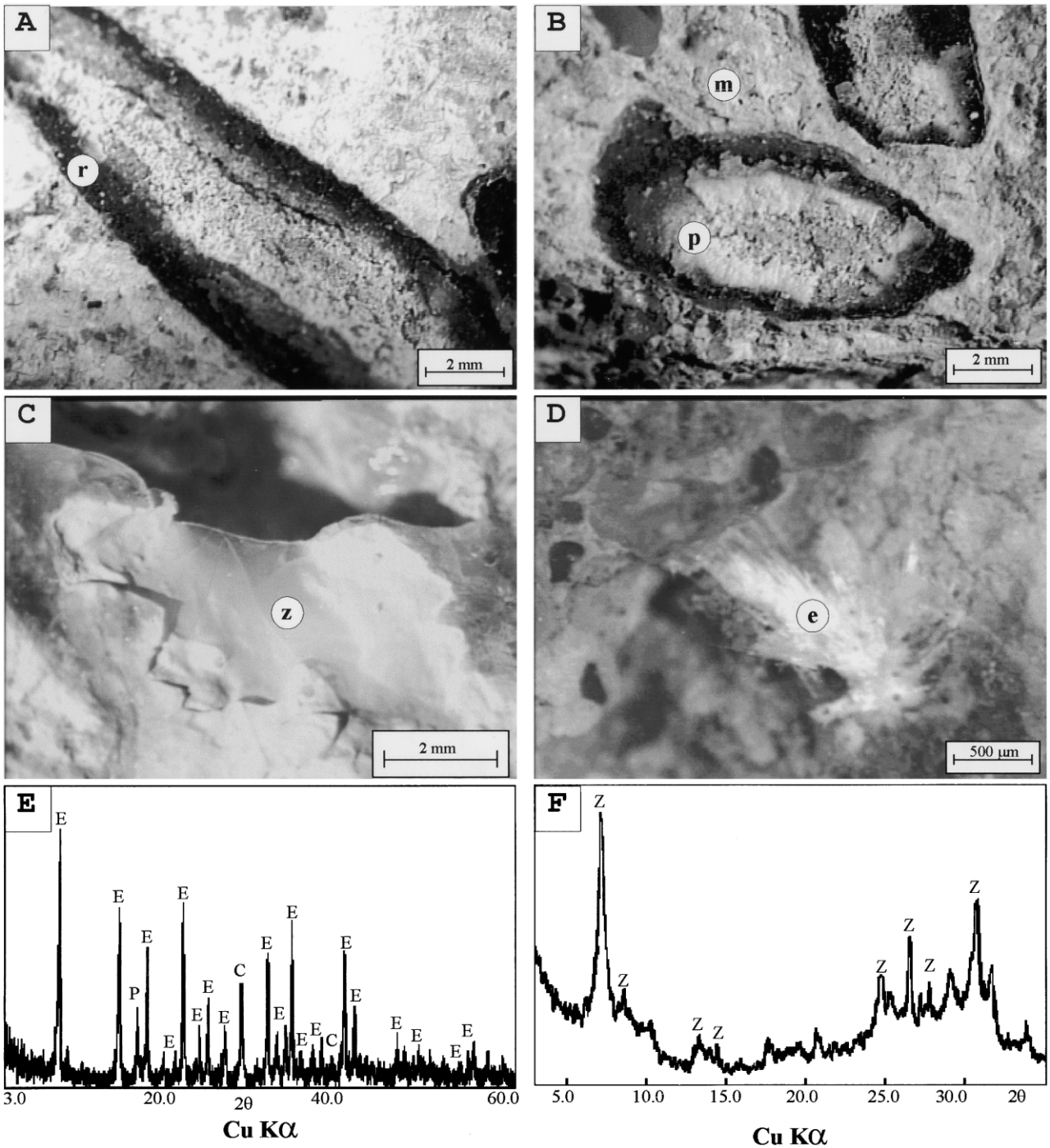

Fig. 1. (A) Coarse aggregate particle with a reaction rim (r). (B) Intense degradation process hat affects the particles (p) and mortar (m). (C) Product of ASR (zeolite, z). (D) Ettringite (e) formation on the concrete surface. (E) XRD of ettringite (E) with portlandite (P) and calcite (C). (F) XRD of the material observed in (C). It corresponds to zeolite (Z) of the erionite group.

aggregate–mortar interface due to the AAR. The fine aggregate contains unweathered volcanic glass as deleterious material.

Concrete B:

The coarse aggregate is composed of granitic migmatite, quartzites, and schists. The three rocks show quartz with undulatory extinction. The fine aggregate contains quartz displaying undulatory extinction (UE angle≅14°).

Concrete C:

City pavement: quartzites (containing microcrystalline quartz with undulatory extinction, UE angle≅11°) and granitic rocks are predominant in the coarse aggregate. The fine aggregate is sand with a high content of glassy vulcanites. Most of the particles show advanced alteration processes. There is also a high content of unweathered volcanic glass. Some glassy vulcanite

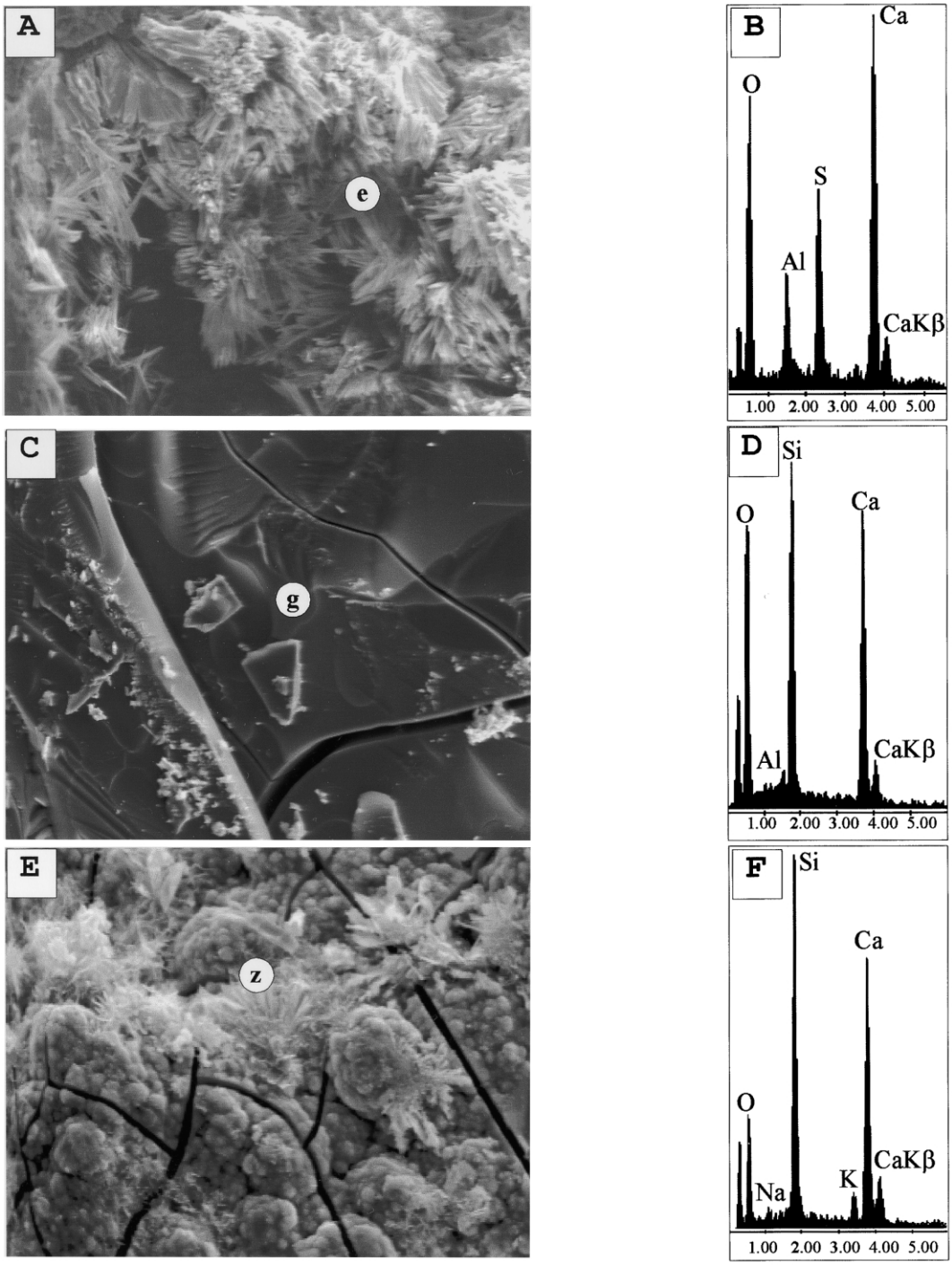

Fig. 2. (A) SEM of ettringite (e) formed inside a cavity. (B) EDAX of the material observed in (A). (C) Product of ASR with a gel-like (g) appearance. (D) EDAX of the material observed in (C). It was identified as Si, Al, O, and Ca. (E) Product of ASR with development of a crystalline habit (zeolite, z). (F) EDAX of (E). Na and K, as well as the abovementioned elements, were identified.

particles have a distinct alteration to argillaceous minerals of the montmorillonite group.

3.4.2. Concrete petrography

The three concretes studied on thin sections show widespread microcracking that affects mainly the mortar and some reactive aggregate particles. Some cracks are filled with an anisotropic material of low birefringence, similar to zeolite. Concrete C exhibits microcracking that, in places, contain AAR product.

If we compare this material with okenite, the latter has a higher refraction index and higher birefringence.

In some cases, it is evident that cracks contain an (isotropic) gel that has partially crystallized.

The reaction process mainly affects the particles of vulcanites and microcrystalline quartz with undulatory extinction. Reaction products were observed to have developed at the aggregate–paste interface.

AAR products were also seen inside entrapped air voids. The voids are filled through microcracks that extend from the reacted particle sites to the voids through the paste phase.

4. Conclusions

1. The deterioration of the three concrete pavements studied is caused by the development of the ASR.

2. The deleterious components are glassy vulcanites, unweathered volcanic glass, and strained and/or microcrystalline quartz.

3. Both AAR gel and crystalline products were identified as the major reaction products. They occurred at the aggregate–mortar interface and inside air voids. Ettringite was also identified in the concrete samples studied, but its significance with respect to the observed damage is unknown.

Acknowledgments

The authors are grateful to the Universidad Nacional del Sur and the Comisión de Investigaciones Científicas de la Provincia de Buenos Aires for their support. They are also indebted to Mr. Rodolfo Salomón for his collaboration in preparing the photomicrographs.

References

[1] P.J. Maiza, S.A. Marfil, C.A. Milanesi, VII Jorn. Pampeanas Cienc. Nat., COPROCNA, Santa Rosa, 1 (1999) 193–200.
[2] P.J. Maiza, S.A. Marfil, O.R. Batic, 9th Int. Conf. Alkali–Aggregate React. Concr., London 2 (1992) 630–637.
[3] S.A. Marfil, P.J. Maiza, Zeolite crystallization in portland cement concrete due to the aliali–aggregate reaction, Cem. Concr. Res. 23 (6) (1993) 1283–1288.
[4] P.J. Maiza, S.A. Marfil, O.R. Batic, Hormigón, Argent. 29 (1996) 11–22.
[5] P.K. Mehta, Mechanism of sulfate attack on portland cement concrete–another look, Cem. Concr. Res. 13 (3) (1983) 401–406.
[6] P.K. Mehta, Concrete: Structure, Properties, and Material, Prentice-Hall, Englewood Cliffs, NJ, 1989.
[7] W.F. Cole, C.J. Lancucki, M.J. Sandy, Products formed in an aged concrete, Cem. Concr. Res. 11 (3) (1981) 443–454.
[8] W.F. Cole, C.J. Lancucki, Products formed in an aged concrete, The occurence of Okenite, Cem. Concr. Res. 13 (5) (1983) 611–618.
[9] S.A. Marfil, P.J. Maiza, G.R. Mas, Segundas Jorn. Geol. Bonaerenses, Bahía Blanca, Argent. 1 (1988) 683–695.
[10] C. Davies, R.E. Oberholsber, 8th Int. Conf. Cem. Microsc. 1 (1986) 303–326.
[11] M.A. Berubé, B. Fournier, Can. Mineral. 24 (1986) 271–288.
[12] International Centre for Diffraction Data (ICDD), Powder Diffraction File, Sets 1–44, 1994.